We are IntechOpen, the world's leading publisher of Open Access books
Built by scientists, for scientists

4,800
Open access books available

122,000
International authors and editors

135M
Downloads

154
Countries delivered to

Our authors are among the

TOP 1%
most cited scientists

12.2%
Contributors from top 500 universities

CLARIVATE ANALYTICS
BOOK CITATION INDEX
INDEXED

WEB OF SCIENCE™

Selection of our books indexed in the Book Citation Index
in Web of Science™ Core Collection (BKCI)

Interested in publishing with us?
Contact book.department@intechopen.com

Numbers displayed above are based on latest data collected.
For more information visit www.intechopen.com

Ultra Wide Band Antenna with Defected Ground Plane and Microstrip Line Fed for Wi-Fi/Wi-Max/DCS/5G/Satellite Communications

Ashish Singh, Krishnananda Shet and Durga Prasad

Abstract

In this chapter, ultra wide band angular ring antenna has been proposed for wireless applications. It has been observed that antenna resonate from 2.9 to 13.1 GHz which has 10.2 GHz bandwidth. Further, it is observed that antenna has nearly omni-directional radiation pattern for E and H-plane at 3.5, 5.8, and 8.5 GHz. The theoretical analysis of the proposed has been done using circuit theory analysis. It was also found using simulation that antenna has good input and output response of 0.2 ns. Proposed antenna measured, simulated, and theoretical results matches for antenna characteristics, i.e., reflection coefficient and radiation pattern. Bandwidth of antenna lies between 2.9 and 13.1 GHz, so this antenna is suitable for Wi-Fi, Wi-Max, digital communication system (DCS), satellite communication, and 5G applications.

Keywords: ultra wide band (UWB), angular ring, finite ground plane, microstrip line fed, circuit theory

1. Introduction

Wireless communication systems are highly desired in various fields of security systems, Wi-Fi, Wi-Max, and mobile communication. These applications have special common devices, i.e., an antenna for efficient transmission and reception information. Presently, antennas are equipped in all communication devices and these devices are size and volume constrains. This leads to reduction of size for antenna in existing communication device. All communication devices have patch antennas for transmission and reception of signals. Scientists and researchers are investigating on these antennas since 1972 for reduction in size and increase in bandwidth. To achieve this, numbers of patch antenna designs and techniques were proposed. It was found by researchers that angular ring patch antenna is an efficient antenna which gives both size reduction and increased bandwidth.

Angular ring patch antenna was first reported in year 1985, by IJ Bahal for biomedical application. Thereafter, only few research have been reported on these antennas such as, theory and experiment on the annular-ring microstrip antenna,

shared aperture microstrip patch antenna array for L and S-Bands, analysis of a gap-coupled stacked annular-ring microstrip antenna, compact stacked circularly polarized annular-ring microstrip antenna for GPS applications, annular-ring microstrip patch antenna with finite ground plane for ultra-wideband applications, compact concentric annular-ring patch antenna for triple-frequency operation, comparison of several novel annular-ring microstrip patch antennas for circular polarization, analysis of two-concentric annular-ring microstrip antenna, and broadband circularly polarized annular-ring microstrip antenna [1–10]. All above reported papers has some limitations such as complicated geometry, lacks theoretical analysis for defected ground with microstrip line feed, circuit diagram at Radio frequency were not proposed for designed antenna and theoretical, simulated and experimental results were not compared.

In this chapter, ultra-wideband microstrip patch antenna is proposed for Wi-Fi, Wi-Max, DCS, and 5G applications. Partial ground plane with microstrip line fed techniques is used to achieve UWB band for various wireless applications. Detail descriptions of proposed antenna design are discussed in next section.

2. Geometrical consideration

The microstrip line fed angular ring patch antenna with rectangular ground is shown in **Figure 1** and the antenna is fabricated on FR$_4$ substrate and its top and bottom view is shown in **Figure 2**. The proposed antenna has been designed on FR$_4$ substrate of height "h" and overall dimension of designed geometry is $(12 \times 14 \times 1.57)$ mm^3. The proposed strip line fed angular ring antenna comprises of ground plane of dimension $(W_G \times L_G)$, and strip line of dimension $(W_L \times L_L)$. Further, antenna is excited via SMA connector fed via strip line. The design specification of complete antenna design is given in **Table 1**. Fabricated antenna picture
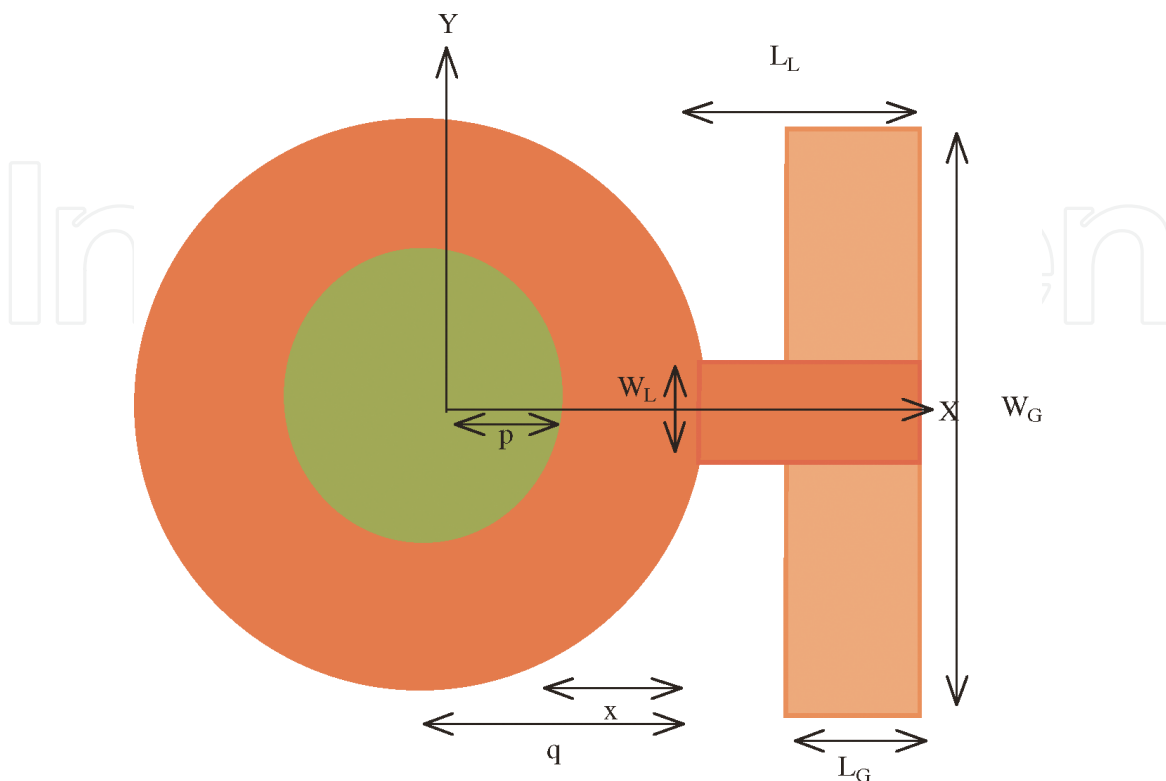

Figure 1.
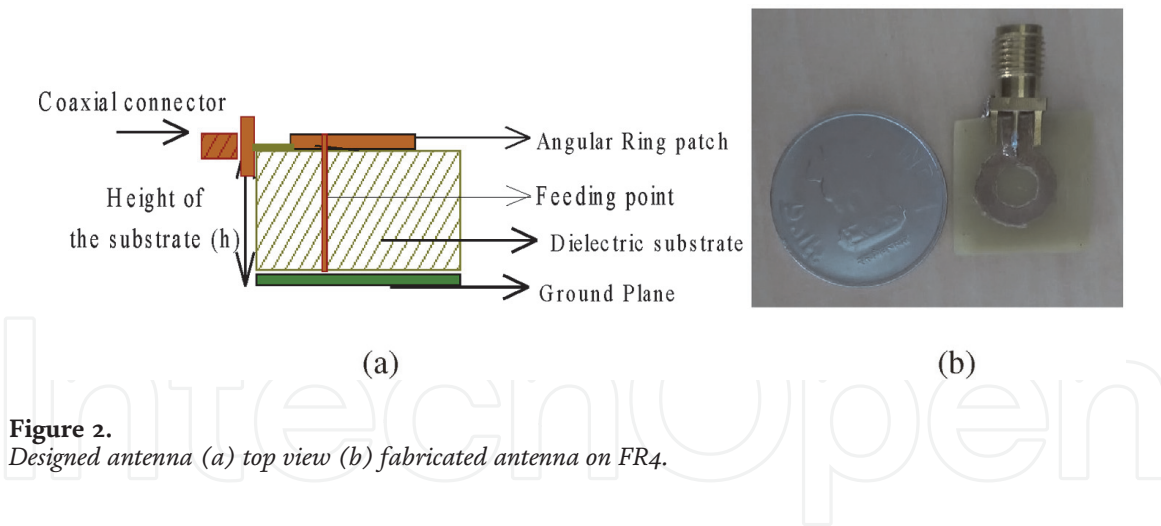*Radiating structure for proposed antenna.*

(a)   (b)

Figure 2.
Designed antenna (a) top view (b) fabricated antenna on FR4.

FR-4 lossy, ε_r	4.4
Radius of angular ring inner, p	3.5 mm
Radius of angular ring outer, q	8.5 mm
Circular path, x	5.0 mm
Strip line length, L_L	5.0 mm
Strip line width, W_L	3.5 mm
Ground plane width, W_G	2.5 mm
Ground plane length, L_G	12 mm
Height of the substrate, h	1.57 mm

Table 1.
Design specification of angular ring antenna.

is shown in **Figure 2(b)**. It can be observed from figure that antenna is very compact in size and can be utilized for compact communication devices.

3. Theoretical investigations

The resonating frequency of angular ring [11] is given as

$$f = \frac{\chi_{nm}}{2\pi p\sqrt{\epsilon_r}}, \tag{1}$$

where c is the velocity of light in free space, $\chi_{nm} = k_{nm}p$, k_{nm} is for the resonant TM_{nm} modes.

The inner and outer radii of angular ring are given as $p_e = p - (x_e - x)/2$ and $q_e = q - (x_e - x)/2$, respectively. The p_e, q_e, and x_e are the effective increase in length of inner, outer, and path width, respectively.

The angular ring patch antenna can be represented in circuit diagram as combination of inductance, capacitance and conductance, as shown in **Figure 3**. The values of inductance L, capacitance C, and conductance G are calculated as.

$$L = \frac{\mu h}{\pi k^2[n,m]}\left[J_n(k_1e)G'_n(k_1p_e) - G_n(k_1e)J'_n(k_1p_e)\right], \tag{2}$$
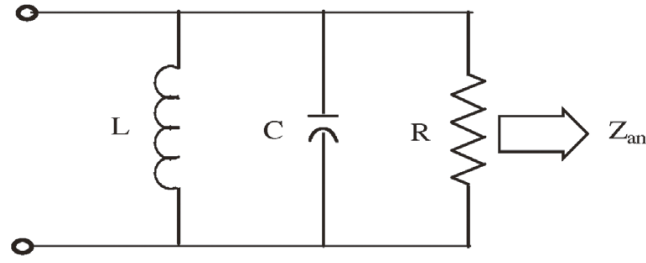
3

Figure 3.
RF circuit representation of angular ring.

$$C = \frac{\mu \epsilon_0 \epsilon_r}{L k_1^2}, \tag{3}$$

$$G = \frac{1}{R} = Re\left[\frac{\pi}{h} \left\{ \left(\frac{E_p}{E_z}\right)^2 g(p,p) + \left(\frac{E_q}{E_c}\right)^2 g(q,q) - \frac{2E_p E_q}{E_z} y(p,q) \right\} \right], \tag{4}$$

where $[n,m] = \frac{1}{2k_1^2} \left[(k_1^2 q_e - 1) \left\{ J_n(k_1 q_e) Y_n'(k_1 p_e) - Y_n(k_1 q_e) J_n'(k_1 p_e) \right\} - \frac{4}{\pi^2 k_1^2 p_e} (k_1^2 q_e^2 - 1) \right]$, $y(p,q)$ is mutual admittance for angular ring between inner and outer radii, $g(p,p)$ is conductance across inner periphery of angular ring, $g(q,q)$ is conductance across outer periphery of angular ring, E_p is the radiation field around inner periphery of angular ring, E_q is the radiation field at outer periphery of angular ring, E_z is the radiation field considered due to ground plane.

Input impedance for the angular ring is given as,

$$Z_{an} = \frac{1}{G + j\omega C + 1/j\omega L}, \tag{5}$$

Angular ring is connected to strip line; the strip line can be represented into RF circuit as combination of L_s, C_s, and Z_0. The RF circuit of the strip line angular patch antenna is shown in **Figure 4**, where L_s and C_s are inductance and capacitance of strip [12, 13].

$$L_s = 100h\left(4\sqrt{W_S/h} - 4.21\right), nH \tag{6}$$

$$C_s = W_s\{(9.5\varepsilon_r + 1.25)W_s/h + 5.2\varepsilon_r + 7.0\}, pF \tag{7}$$
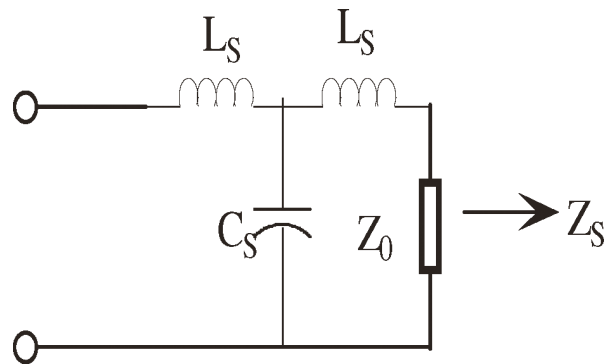

Figure 4.
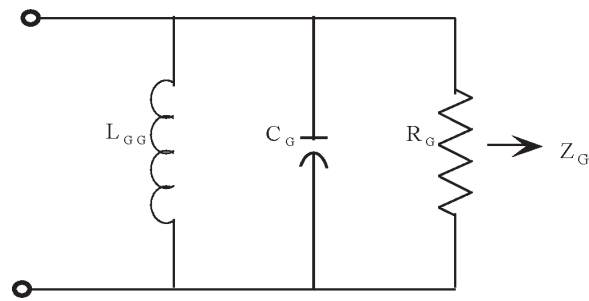*RF circuit diagram for strip line.*

Figure 5.
RF circuit representation for ground plane.

The resonating frequency of the strip line is given as

$$f = c/2L_{se}\sqrt{\varepsilon_{re}},\tag{8}$$

The ground plane patch is represented as RF circuit combination of Resistance R_G, inductance L_{GG}, and capacitance C_G. The RF circuit representation of the ground plane is shown in **Figure 5**, R_G, C_G, L_{GG} can be calculated as [12, 13].

$$C_G = \frac{L_G W_G \varepsilon_0 \varepsilon_e}{2L_G}\cos^2\left(\frac{\pi}{L_G}\right),\tag{9}$$

$$R_G = \frac{Q}{\omega_r^2 C_G},\tag{10}$$

$$L_{GG} = \frac{1}{C_G \omega_r^2},\tag{11}$$

$$\text{Quality factor}, Q = \frac{c\sqrt{\varepsilon_e}}{4fh}.\tag{12}$$

ε_e is the effective permittivity of the medium.

Further, there will be strong electromagnetic field between top patch (i.e., angular ring and strip line) and ground plane (rectangular patch). Due to which inductance and capacitance are developed between them and its RF circuit representation is shown in **Figure 6**. Thereafter, on excitation of antenna the impedance is also developed between top and bottom patch [12–14] and represented as,

$$Z_{ee} = 1/\left[\frac{1}{j\omega L_{ee}} + j\omega C_{ee}\right]\tag{13}$$

$$L_{ee} = \frac{L_g \times L_{an}}{L_g + L_{an}} + L_{gan},\tag{14}$$
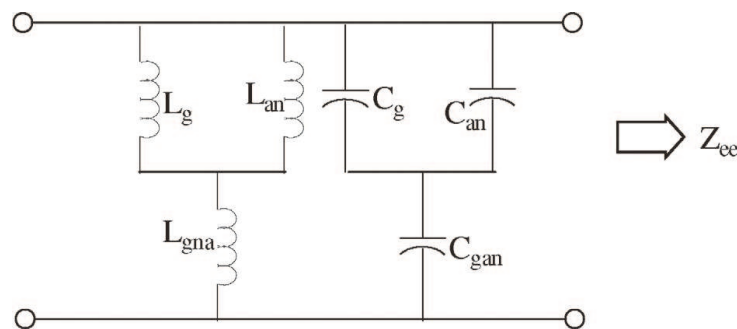

Figure 6.
RF circuit diagram of electromagnetically coupled between ground plane and radiating patch.

$$C_{ee} = \frac{(C_g + C_{an}) \times C_{gan}}{C_g + C_{an} + C_{gan}} \tag{15}$$

L_{ee} and C_{ee} are the equivalent inductance and capacitance developed because of electromagnetic coupling.

L_{an} and C_{an} are electromagnetically developed mutual inductance and capacitance for angular ring.

$$L_{gan} = \frac{k_{gc}^2 (L_g + L_{an}) + \left[k_{gc}^4 (L_g + L_{an})^2 + 4k_{gc}^4 \left(1 - k_{gc}^2\right) L_g L_{an} \right]^{1/2}}{2\left(1 - k_{gc}^2\right)}, \tag{16}$$

$$C_{gan} = \frac{-(C_g + C_{an}) + \left[(C_{an} + C_g)^2 + \left(1 - 1/k_{gc}^2\right) C_{an} C_g \right]^{1/2}}{2}, \tag{17}$$

$$k_{gc} = \frac{1}{\sqrt{Q_g Q_{gg}}}, \tag{18}$$

$$Q_g = R_G \sqrt{\frac{C_G}{L_{GG}}}, \tag{19}$$

$Q_{gg} = R_{an} \sqrt{\frac{C_{an}}{L_{an}}}$, Q_g and Q_{gg} are quality factor for both the resonators, R_{an} impedance of microstrip.

The input impedance of strip line feed angular ring with defected ground plane and its RF circuit representation is shown in **Figure 7** and is calculated using Eqs. (2)–(19)

$$Z_{in} = \frac{1}{\frac{1}{Z_G} + \frac{1}{Z_s} + \frac{1}{Z_{an}} + \frac{1}{Z_{ee}}} \tag{20}$$

Using Eq. (20) the input impedance of proposed has been used to calculate reflection coefficient (RC), return loss (RL) and voltage standing wave ratio (VSWR) can be calculated as,

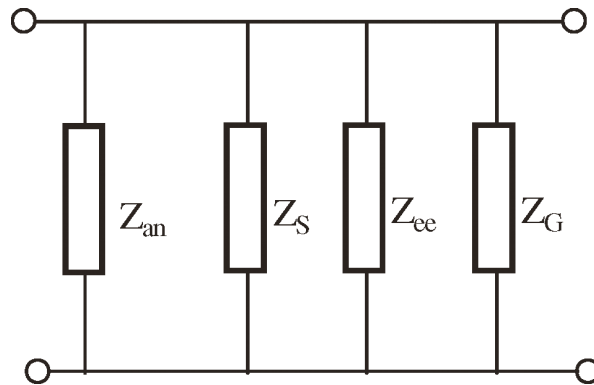$$\text{Reflection Coefficient } \Gamma = \frac{Z - Z_{in}}{Z + Z_{in}}, \tag{21}$$

Figure 7.
The equivalent RF circuit diagram of microstrip angular patch antenna.

where Z is the input impedance of the microstrip fed (*50 Ω*).

$$VSWR = \frac{1 + |\Gamma|}{1 - |\Gamma|}, \tag{22}$$

$$\text{Return loss (RL)} = 20 \log |\Gamma| \tag{23}$$

Using Eqs. (21)–(23) the theoretical plots for RL, VSWR, and RC with respect to frequency (GHz) can be plotted. In this chapter, theoretical plot for RC with respect to frequency (GHz) is plotted.

4. Result and discussion

The comparison between simulated [14], measured, and theoretical results is shown in **Figure 8(a)**. It is observed from the figure that these three results are in approximately close with each other. Further, the bandwidth of theoretical, measured and simulated results is 10.63, 10.6, and 10.2 GHz, respectively. Bandwidth of antenna lies between 2.9 and 13.1 GHz, these bands are suitable for Wi-Max, Wi-Fi,
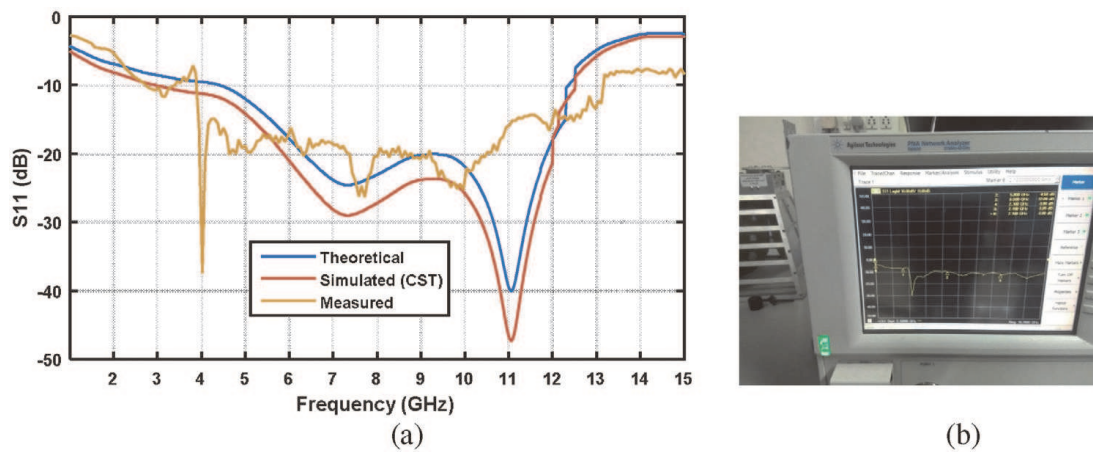
Figure 8.
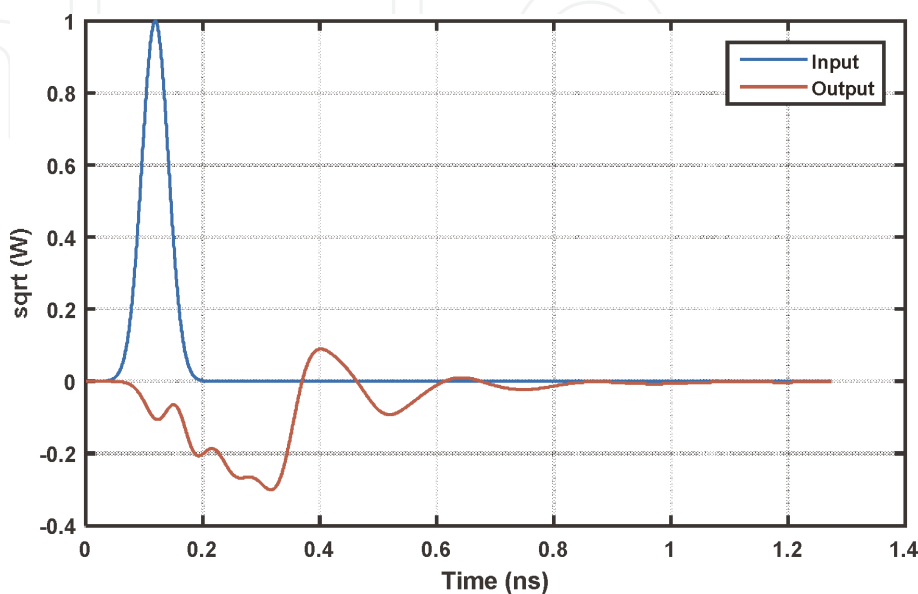*(a) Comparative results of proposed antenna; (b) measured result on VNA.*

Figure 9.
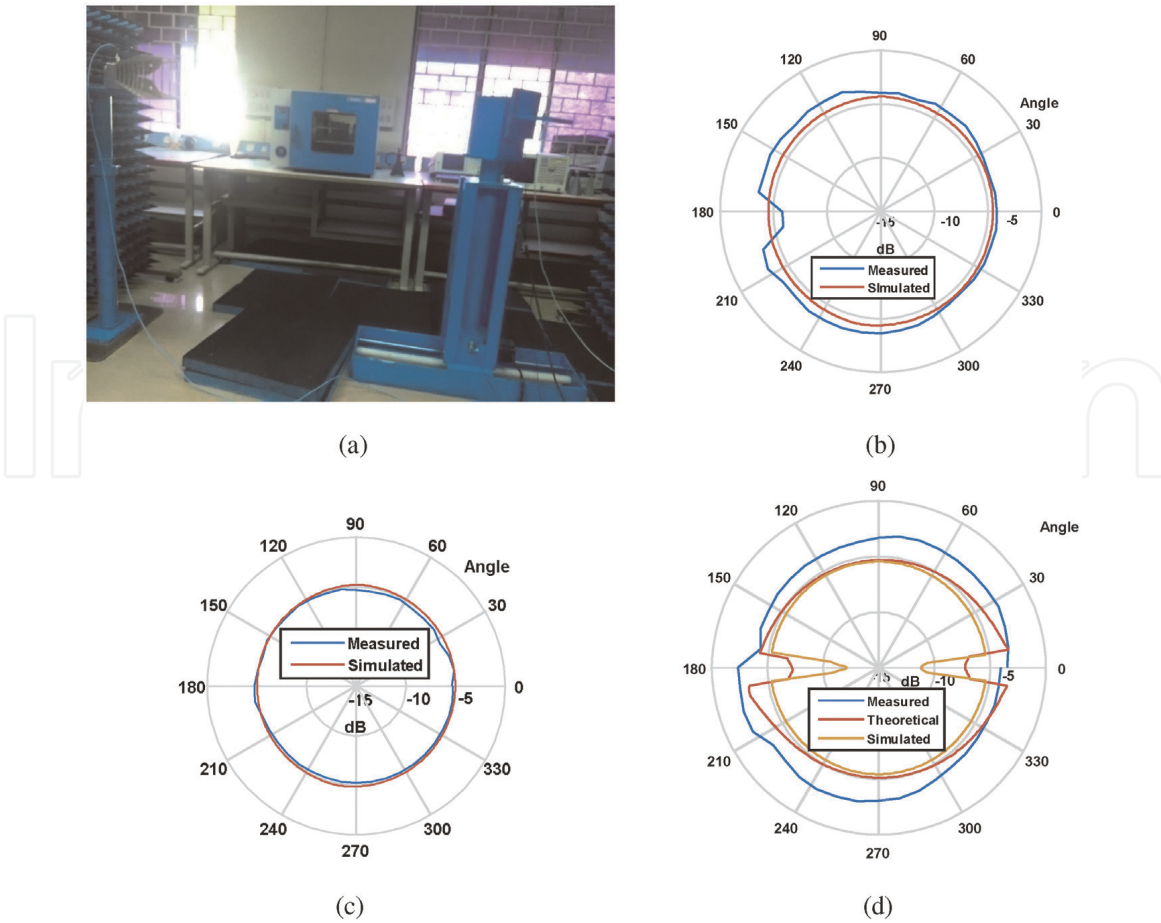*Input and output response for the excited proposed antenna.*

(a)

(b)

(c)

(d)

Figure 10.
Radiation pattern for H-plane (a) anechoic chambers with antennas; (b) 3.5 GHz, (c) 5.8 GHz, and
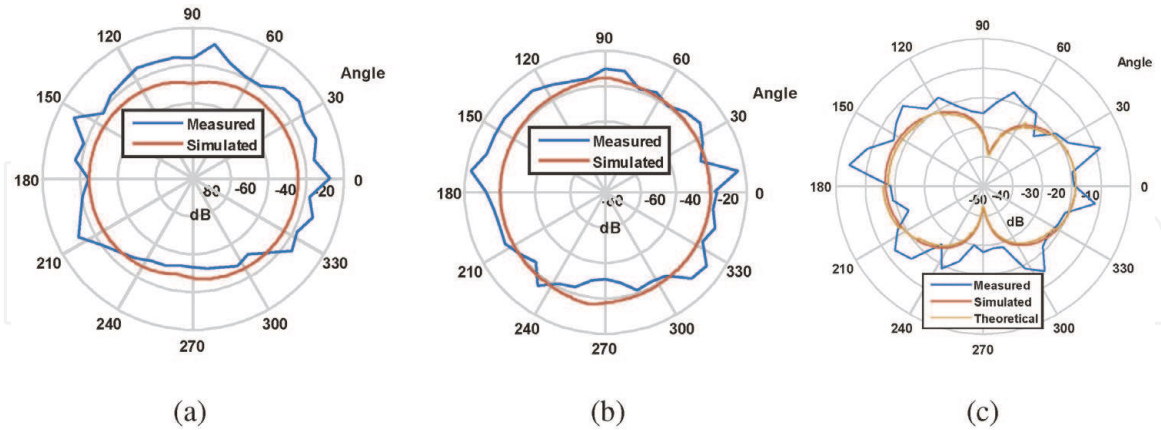*(d) 8.5 GHz.*

(a)

(b)

(c)

Figure 11.
Radiation pattern for E-plane (a) 3.5 GHz, (b) 5.8 GHz, and (c) 8.5 GHz.

digital communication system, satellite communication, and 5G applications. Measured result picture on Vector Network Analyzer (VNA) of proposed antenna is shown in **Figure 8(b)**.

From **Figure 9**, it is observed that maximum input amplitude of the antenna is 1 sqrt W at 0.1 ns time interval, whereas maximum output amplitude is 0.34 sqrt W at a response time of 0.38 ns with phase reversal. The output response is not smooth because angular ring structure with rectangular ground plane.

Radiation pattern of the proposed antenna are shown in **Figures 10** and **11** for E and H-plane, respectively. **Figure 10(a)** shows the radiation pattern measurement setup, proposed antenna under test is kept 200 cm apart from the horn antenna. **Figure 10(b)** and **(c)** are measured and simulated radiation pattern at 3.5 and 5.8 GHz, respectively. Measured and simulated radiation pattern are in close agreement in both cases and omni-directional patterns are observed. **Figure 10(d)** shows radiation pattern at center frequency. Major and minor lobes have been observed of same beam width for measured, theoretical, and simulated antenna at center frequency 8.5 GHz for H-plane. **Figure 11(a)–(c)** shows the radiation pattern for E-plane at 3.5, 5.8, and 8.5 GHz, respectively. Antenna shows nearly omni-directional radiation pattern at 3.5 and 5.8 GHz; whereas at 8.5 GHz, it is partially eight shaped. Electric field intensity is more toward 180° for E-plane and antenna 3 dB beam width is 87.4°. Slightly mismatch is observed in radiation pattern results because of partially open anechoic chambers and fabrication defects. It has omni-directional pattern so this antenna can be utilized for mobile communication.

Figures 12–14 show the surface current distribution of proposed antenna at center frequency for 90 and 0° phase, respectively. Further, from **Figure 12**, the
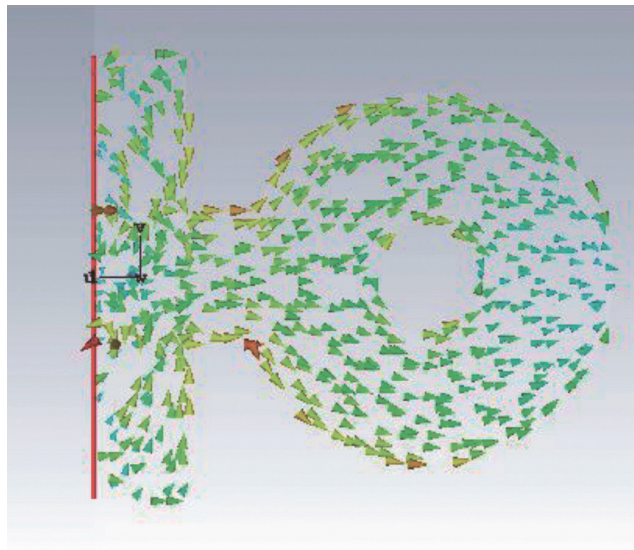

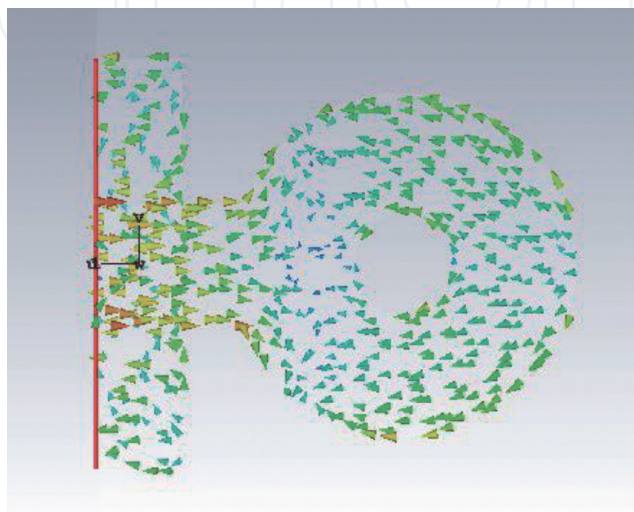**Figure 12.**
Current distribution at 90° phase.

Figure 13.
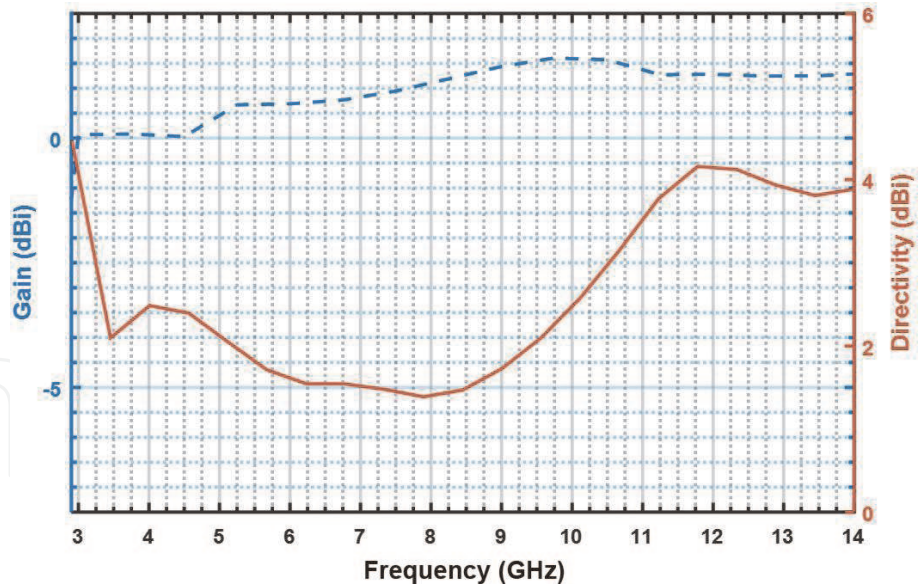*Current distributions at center frequency at 0° phase.*

Figure 14.
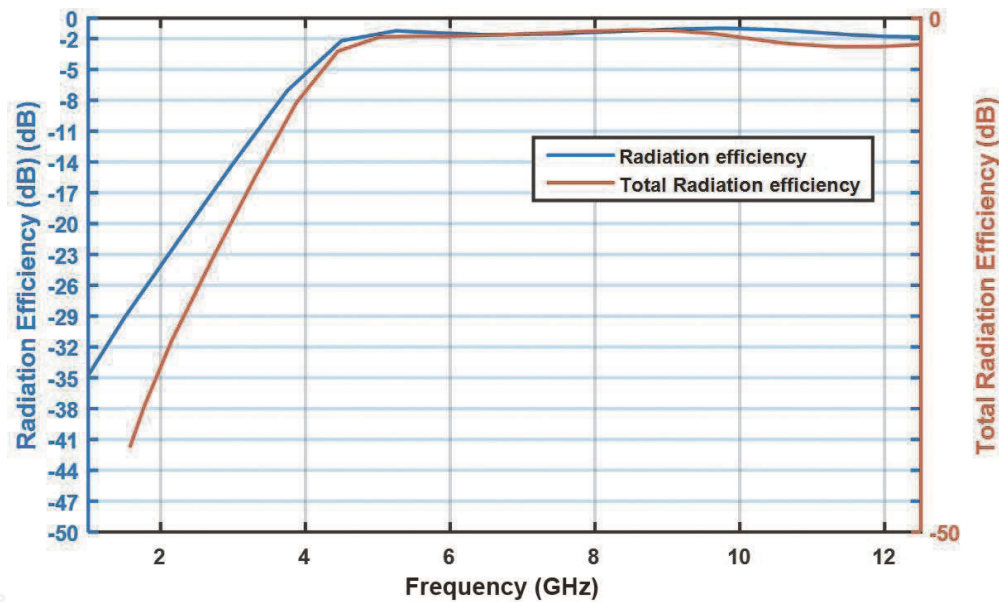*Gain and directivity of proposed antenna.*

Figure 15.
Radiation efficiency of proposed antenna.

maximum surface current of 86.4766 A/m is observed at the outer perimeter of angular ring near the edges of strip line and surface current is evenly distributed along length of antenna at 90° phase. Whereas, the surface current at 0° phase is not evenly distributed along the length of antenna and more surface current observed near feed as shown in **Figure 13**.

Figure 14 shows the gain and directivity of the antenna in dBi. It is observed that maximum gain of 2.75 dBi is achieved at 10.2 GHz; whereas, average gain of antenna is 2.1 dBi. Further, the directivity of the antenna at 10.2 GHz is maximum, i.e., 4.1 dBi and average directivity is 2.98 dBi.

The maximum radiation efficiency is achieved −1.5 dB (70.79%) at 10.2 GHz frequency as observed in **Figure 15** and total radiation efficiency of proposed antenna at 10.2 GHz is found to be (−2.2 dB) 60.25%. This is because the loss occurs due to skin effect and conduction loss in antenna device.

5. Conclusion

From the above theoretical analysis, it is found that angular ring patch antenna can be utilized for UWB antenna. Further was observed that antenna cover frequency band between 2.9 and 13.1 GHz which has 125% bandwidth. From the results, it was also observed that antenna has good radiation characteristics and input and output response. Antenna has the gain and efficiency of 2.2 dBi and 70.79%. Simulated, measured, and theoretical results are matching for radiation pattern and reflection coefficient. Further, this antenna is suitable for digital communication system, satellite communication, and 5G applications.

Acknowledgements

Author details

Ashish Singh*, Krishnananda Shet and Durga Prasad
Department of Electronics and Communication Engineering, N.M.A.M. Institute of Technology (Affiliated to Visvesvaraya Technological University, Belagavi) Nitte, Udupi, Karnataka, India

*Address all correspondence to: ashsin09@rediffmail.com

IntechOpen

References

[1] Lee KF, Dahele JS. Theory and experiment on the annular-ring microstrip antenna. Annales des Telecommunications. 1985;**40**:508-515

[2] Dhiman J, Sharma A, Khah SK. Shared aperture microstrip patch antenna array for L and S-bands. Progress in Electromagnetics Research Letters. 2019;**86**:91-95

[3] Ansari JA, Ram RB, Singh P. Analysis of a gap-coupled stacked annular ring microstrip antenna. Progress in Electromagnetics Research B. 2008;**4**: 147-158

[4] Ding K, Yu T-B, Zhang Q. A compact stacked circularly polarized annular-ring microstrip antenna for GPS applications. Progress in Electromagnetics Research Letters. 2013;**40**:171-179

[5] Rawat S, Sharma KK. Annular ring microstrip patch antenna with finite ground plane for ultra-wideband applications. International Journal of Microwave and Wireless Technologies. 2015;**7**(2):179-184

[6] Bao XL, Ammann MJ. Compact concentric annular-ring patch antenna for triple-frequency operation. Electronics Letters. 2006;**42**:1129-1130

[7] Bao XL, Ammann MJ. Comparison of several novel annular-ring microstrip patch antennas for circular polarization. Journal of Electromagnetic Waves and Applications. 2006;**20**:1427-1438

[8] Kanaujia BK, Vishvakarma BR. Analysis of two-concentric annular ring microstrip antenna. Microwave and Optical Technology Letters. 2003;**36**: 104-108

[9] Guo Y-X, Bian L, Shi XQ. Broadband circularly polarized annular-ring microstrip antenna. IEEE Transactions on Antennas and Propagation. 2009;**57**: 2474-2477

[10] Rasool N, Kama H, Basit MA, Abdullah M. A low profile high gain ultra lightweight circularly polarized annular ring slot antenna for airborne and airship applications. IEEE Access. 2019;**7**:155048-155056

[11] Kumar G, Ray KP. Broadband Microstrip Antenna. USA: Artech House; 2003

[12] Bahal IJ, Bartia P. Microstrip Patch Antenna. USA: Artech House; 1980

[13] Meada M. Analysis of gap in microstrip transmission line. IEEE Transactions on Antennas and Propagation. 1972;**32**:1375-1379

[14] Computer Simulation Technology (CST). Microwave Studio Suite Version. Germany: Dassault Systèmes and Darmstadt; 2018